RSC Advances

PAPER

View Article Online
View Journal | View Issue

Cite this: *RSC Adv.*, 2023, **13**, 32137

A fluorous-tag-assisted fluorescent probe for simple and selective detection of hydrogen sulfide: application for turbid dyeing solutions†

Geonwoo Park,‡ Mincheol Jang‡ and Min Su Han *

Accurate hydrogen sulfide (H_2S) detection has attracted much attention because its toxicity may affect aquatic environments and human health. However, recognizing H_2S levels by conventional fluorescent probes in turbid wastewater has been challenging because the opaque environment interferes with their photophysical properties. To overcome this limitation, a fluorous-tagging strategy can be used for the development of fluorescent sensors to detect H_2S in turbid solutions. The use of fluorescent probe assisted with fluorous-tag allowed for easy isolation of the probe using polytetrafluoroethylene (PTFE) material, while disturbing species were eliminated through a simple aqueous wash. This approach enabled the fluorescent probe to effectively quantify H_2S, even in opaque solutions containing organic dyes that could interfere with fluorescence emission.

Received 4th October 2023
Accepted 20th October 2023

DOI: 10.1039/d3ra06740h

rsc.li/rsc-advances

1 Introduction

Hydrogen sulfide (H_2S) is a toxic gas with a strong odor of rotten eggs that has been recognized as an endogenous gasotransmitter with nitric oxide (NO) and carbon monoxide (CO).[1–4] Sulfide compounds are commonly used and produced in industrial plants such as bleach in paper, printing, and dye production industries.[5,6] Especially, H_2S in wastewater can cause undesirable corrosions of metals in aquatic environments such as rivers, resulting in harmful effects on physiological processes and life activities of human health.[7,8] Hence, the detection of H_2S in industrial wastewater has been widely recognized as an invaluable technique in recent decades.

Many approaches to detect H_2S using gas chromatography, colorimetry, and electrochemical method, have been suggested.[9–11] However, many of these approaches are often limited and avoided owing to their high costs, time-consuming procedures, and complex processes.[12,13] The fluorescent method for H_2S detection has gained significant attention owing to its high sensitivity, non-invasiveness, rapid response, and simplicity.[14,15] However, the application of the fluorescent method is limited for certain real samples in terms of interference because fluorescence is easily affected by the environment of samples.[16,17] Hence, it is important to design the fluorescent probe so that it can effectively work regardless of interfering species. As representative examples, various research groups have introduced special functionalities to the fluorescent probe to enhance the probe's selectivity for target analyte or prevent the overlap of emission ranges with interfering fluorescence.[18–21] Nevertheless, the use of the fluorescent probes in deep-coloured solution, such as dyeing wastewater, remains challenging because the strong light scattering and light absorption induced by the turbid media can significantly attenuate the fluorescence intensity.[22,23] Therefore, a new alternative is required to develop a fluorescent probe that can accurately detect analytes independent of solution color and turbidity.

From this perspective, the fluorous-tagging strategy offers a solution by allowing for the easy and rapid isolation of the fluorescent probe, thereby minimizing interferences from other disturbing species.[24] A fluorous-tag is a simple and long perfluoroalkyl chain moiety; thus, fluorous-tag-assisted substrates have strong, specific fluorous interaction with polytetrafluoroethylene (PTFE) materials, such as PTFE particles.[25–27] This specific affinity enables the fluorous-tagged substrates to be readily isolated using fluorous solid-phase extraction (F-SPE), eliminating the need for pre-filtration, column chromatography, recrystallization, and other troublesome purification procedures.[27,28] Despite these advantages, there have been few research applying the fluorous-tagging strategy in the field of chemosensors.[29] Therefore, a combination of fluorous-tag and fluorescent probe is expected to be an efficient new approach to the detection of targets in deep-coloured solutions.

In this study, a fluorous-tagged naphthalimide derivative, **F-Naph-N_3** was used as a fluorescent probe for quantitatively

Department of Chemistry, Gwangju Institute of Science and Technology (GIST), 123 Cheomdangwagi-ro, Buk-gu, Gwangju 61005, Republic of Korea. E-mail: happyhan@gist.ac.kr

† Electronic supplementary information (ESI) available: Characterization data, photophysical properties, and experimental details for H_2S sensing in fluorescence spectrophotometer and imaging instrument. See DOI: https://doi.org/10.1039/d3ra06740h

‡ Geonwoo Park and Mincheol Jang contributed equally.

detecting H_2S (Scheme 1). It also showed good selectivity and competitive selectivity for H_2S in solution. Furthermore, this probe has highly hydrophobic and fluorophilic properties owing to the fluorous-tag, and it can thus be easily separated from commercially available PTFE materials through two simple steps: (1) spotting the sample on a PTFE membrane filter and (2) washing the membrane with deionized water (Scheme 1b). The sample solution containing **F-Naph-N$_3$** and H_2S spotted on PTFE membrane filter exhibited intense fluorescence, allowing for quantification of the H_2S amount using imaging instrument. Finally, **F-Naph-N$_3$** was successfully used as a sensor to detect H_2S in dye-containing opaque solutions, which is hard to achieve using conventional fluorescent probes and spectrometers.

2 Experimental

2.1 Materials and instruments

All chemical reagents were purchased from commercial suppliers (TCI, Sigma-Aldrich, Combi-blocks, DUKSAN and DAEJUNG). Except for 4-bromo-1,8-naphthalic anhydride, all reagents were used without any pre-purification. Polytetrafluoroethylene (PTFE) membrane filter was purchased from Advantec.

Proton nuclear magnetic resonance (400 MHz for ^{1}H NMR), carbon NMR (100 MHz for ^{13}C NMR), fluorine NMR (376 MHz for ^{19}F NMR) spectra were obtained using a JEOL (400 MHz) NMR spectrometer. All UV/Vis spectra were recorded using an JASCO V-630 UV/Vis spectrometer, and all fluorescence spectra were measured using an Agilent Cary Eclipse fluorescence spectrometer. High-resolution mass spectra (HRMS) were obtained at Korea Basic Science Institute (Daegu, South Korea) using a JEOL KMS-700 MStation mass spectrometer with a standard electron ionization (EI+) source or fast atom bombardment (FAB+) ion source. Melting points were measured using a BUCHI melting point M-565 apparatus. All Fluorescence images of PTFE membrane were visualized using a ChemiDoc MP imager (Bio-Rad) which was set as following – exposure time 0.01 s, excitation source: blue epi illumination, emission filter: 530/28 filter. Their fluorescence intensities were converted into green value (optical density) by using an Adobe Photoshop software.

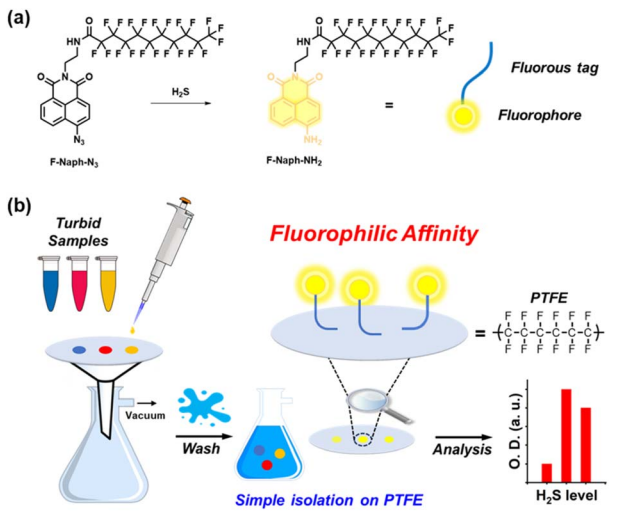

Scheme 1 (a) Schematic of H_2S detection by F-Naph-N$_3$ based on naphthalimide fluorophore. (b) Graphical abstract illustrating the application of F-Naph-N$_3$ for H_2S detection in turbid dyeing samples by polytetrafluoroethylene (PTFE) membrane filter.

2.2 Synthesis of 6 and F-Naph-N$_3$

Heneicosafluoroundecanoic acid (1.35 g, 2.4 mmol), thionyl chloride (2.9 mL, 40.0 mmol), and pyridine (19.2 μL, 0.24 mmol) were refluxed for 4 h. Thionyl chloride was removed under reduced pressure to give **6** as a white solid, and **6** was used in further reaction. To the next, **5** (0.42 g, 1.5 mmol) and triethylamine (0.25 g, 1.8 mmol) were dissolved in 24 mL of dry tetrahydrofuran (THF) and then **6** was added to the reaction mixture. The mixture was stirred for 24 h at room temperature. After the reaction, 100 mL of water was poured into the reaction mixture, and the precipitated solid was filtered. The residue was dissolved in DCM, washed with brine, dried over Na_2SO_4, and the solvent was evaporated under reduced pressure. The collected solid was further purified by silica gel column chromatography (chloroform : methanol = 50 : 1 as an eluent) to afford **F-Naph-N$_3$** (0.30 g, 24%) as a yellow solid. ^{1}H NMR (400 MHz, $CDCl_3$, δ, ppm): 8.66–8.68 (dd, J = 7.2, 1.2 Hz, 1H), 8.60–8.62 (d, J = 8.0 Hz, 1H), 8.48–8.50 (dd, J = 8.4, 1.2 Hz, 1H), 7.75–7.79 (dd, J = 8.4, 7.6 Hz, 1H), 7.51 (br s), 7.48–7.50 (d, J = 11.6 Hz, 1H), 4.48–4.51 (m, 2H), 3.77–3.81 (q, J = 4.8 Hz, 2H). ^{13}C NMR (100 MHz, $CDCl_3$, δ, ppm): 164.93, 164.47, 157.99, 144.37, 132.89, 132.43, 129.56, 129.32, 127.05, 124.47, 121.98, 118.15, 114.84, 40.70, 38.69 (carbon peak of fluorous-tag could not be observed due to low solubility and signal). ^{19}F NMR (376 MHz, $CDCl_3$, δ, ppm): −80.61, −119.64, −121.52, −121.70, −122.52, −122.58, −125.99. Melting point: 154–163 °C. HRMS (FAB+): m/z calculated for $C_{25}H_{11}F_{21}N_5O_3$ + H^+ [M + H^+]: 828.0527, found: 828.0530.

2.3 General and pH dependence

All sample solutions (1.0 mL) were prepared in 1.5 mL Eppendorf tube. All fluorescence measurements were repeated three times at room temperature. To test the pH dependence of probe, H_2S (60 μM) was added to various buffer solutions (10 mM, pH 4.0–10.0) containing **F-Naph-N$_3$** (20 μM, 60% ACN). The fluorescence spectra were measured after 1 h. λ_{ex} = 418 nm. λ_{em} = 530 nm. Slit widths: 5 nm. The composition of buffer solution were as follows: pH 4.0–5.0 (sodium acetate), pH 6.0 (2-(*N*-morpholino)ethanesulfonic acid, MES), pH 7.0–8.0 (sodium phosphate), pH 9.0 (tris(hydroxymethyl)aminomethane, Tris), pH 10.0 (sodium bicarbonate).

2.4 Selectivity and competitive selectivity of F-Naph-N$_3$ toward H_2S over other anions/biothiols

Various anions/biothiols (100 μM, CO_3^{2-}, HCO_3^-, CH_3COO^-, Cl^-, F^-, Br^-, I^-, NO_2^-, NO_3^-, N_3^-, SO_3^{2-}, SO_4^{2-}, HSO_4^-, CN^-/Cys, Hcy, and GSH) were added to sodium phosphate buffer

solution (SPB, 10 mM, pH 8.0) containing **F-Naph-N_3** (20 μM, 60% ACN). H_2S (100 μM) and same anions/biothiols (300 μM) as in selectivity test were added to sodium phosphate buffer solution (SPB, 10 mM, pH 8.0) containing **F-Naph-N_3** (20 μM, 60% ACN). The fluorescence spectra were obtained after 1 h. λ_{ex} = 418 nm. λ_{em} = 530 nm. Slit widths: 5 nm.

2.5 Quenching effect by copper nitrate trihydrate

The different concentrations of H_2S (20, 40, and 60 μM) were added to sodium phosphate buffer solution (SPB, 10 mM, pH 8.0) containing **F-Naph-N_3** (20 μM, 60% ACN), and fluorescence intensity was measured for 1 h. Copper nitrate trihydrate (2 eq. of added H_2S, 2 vol%) was then added to the solution, followed by additional measurement for 30 min. λ_{ex} = 418 nm. λ_{em} = 530 nm. Slit widths: 5 nm.

2.6 Practical application for dyeing samples

Alizarin red S (150 μM), bromophenol blue (150 μM), methyl orange (150 μM), and their triple mixture (50 + 50 + 50 μM) were prepared as opaque environments for the dyeing solutions. Each concentration of H_2S (20, 40, and 60 μM) was added to SPB (10 mM, pH 8.0) containing **F-Naph-N_3** (20 μM, 60% ACN) and organic dyes. After the incubation for 1 h, copper nitrate trihydrate (2 eq. of added H_2S, 2% v/v) was added to the sample to quench the reaction. 5 μL of sample was spotted onto PTFE membrane filter, and then water (80 mL × 2) was filtered to wash buffer, organic dyes, and other species, except for the probe. The wet PTFE membrane was dried up quickly by cool air-blowing. The fluorescence intensity was visualized using ChemiDoc MP imager (Bio-Rad) and then converted into optical density value using Adobe Photoshop software.

3 Results and discussions

3.1 Design and photophysical properties of probe

To design the fluorescent probe, a 1,8-naphthalimide scaffold was selected as a fluorophore because of its high quantum yield, good stability and solubility, low cost, and variable synthetic modification.[30,31] A 4-positioned azide in naphthalimide was set as detecting group, which can be selectively reduced to amine by H_2S, thereby inducing fluorescence of probe. Finally, the –$C_{10}F_{21}$ fluorous-tag was introduced through an *N*-(2-aminoethyl) acetamide moiety as a linker and **F-Naph-N_3** was successfully synthesized (Scheme S1†). As shown in Scheme 1a, **F-Naph-N_3** encounting H_2S exhibited intense fluorescence turn-on upon conversion into **F-Naph-NH_2**. To confirm the photophysical properties, the UV/Vis spectra of **F-Naph-N_3** and **F-Naph-NH_2** in acetonitrile (ACN) were investigated to verify their absorption properties. **F-Naph-N_3** showed a maximum absorption peak at 365 nm while **F-Naph-NH_2** showed a red-shifted absorption at 418 nm (Fig. S1†).

3.2 Screening experiments for optimization

Several screening experiments were conducted to optimize detection condition. First, solvent screening was examined and ACN was chosen because it had both appropriate solubilities to highly hydrophobic **F-Naph-N_3** and miscibility with H_2O which accommodates buffer, H_2S and quenching agent. Furthermore, the high volatility of ACN was suitable for application in F-SPE. Notably, ACN/H_2O (v/v = 6 : 4) was determined to be the optimal solvent because the salt precipitated at an H_2O ratio of less than 40%.

Next, the kinetics of **F-Naph-N_3** with H_2S were also studied.

Time-dependent fluorescence spectra were measured 2 h after the addition of various concentrations of H_2S (Fig. 1b). Upon the addition of H_2S, a gradual increase in the peak at 530 nm was observed over time. The fluorescence intensity enhancement was relatively moderate after 1 h for all H_2S concentrations.

Moreover, the effects of the pH on the sensing reaction and fluorescence activity were also investigated. Fluorescence spectra of probe **F-Naph-N_3** (20 μM) were monitored in the presence and absence of H_2S (3 eq.) at pH from 4.0 to 10.0 (Fig. 1c). The fluorescence intensity without H_2S was negligible in all pH ranges, and despite the addition of H_2S, the probe exhibited little fluorescence in the acidic pH range (pH < 7.0). The fluorescence sharply increased at a neutral pH and gradually increased as the pH increased. Hence, sodium phosphate buffer (SPB, pH 8.0) was selected as the optimized pH for experiment, which is close to physiological environment and provides sufficient fluorescence activity.

3.3 Sensitivity and selectivity of F-Naph-N_3 toward H_2S

H_2S titration experiments were conducted under optimized conditions to determine the sensing performance of **F-Naph-N_3** for H_2S. The probe (20 μM) was incubated for 1 h in SPB (10 mM, pH 8.0) and ACN/H_2O (v/v = 6 : 4) solutions after the addition of H_2S, and the fluorescence spectra were measured (Fig. 1d). Before the addition of H_2S, there was little fluorescence intensity; however, the peak at 530 nm was enhanced in proportion to the increasing H_2S concentration. **F-Naph-N_3** can detect H_2S quantitatively with a detection limit as low as 0.28 μM (Fig. S2†).

To examine the selectivity of **F-Naph-N_3** for H_2S among various interfering species, fluorescence spectra of the probe (20 μM) were measured with 100 μM of H_2S and several biothiols (Cys, Hcy, and GSH) and various anions (CO_3^{2-}, HCO_3^-, CH_3COO^-, Cl^-, F^-, Br^-, I^-, NO_2^-, NO_3^-, N_3^-, SO_3^{2-}, SO_4^{2-}, HSO_4^- and CN^-). Most analytes, except for H_2S, rarely contribute to fluorescence enhancement (Fig. 1e). Furthermore, when **F-Naph-N_3** (20 μM) was treated with H_2S (100 μM) and same analytes (300 μM) as in the previous test, the interference of other analytes on the sensing system was almost negligible (Fig. 1f). Both experiments demonstrate that **F-Naph-N_3** affords good selectivity and competitive selectivity for H_2S.

3.4 Fluorous solid-phase extraction using F-Naph-N_3

Before applying **F-Naph-N_3** in F-SPE, copper nitrate was introduced as a H_2S scavenger after the incubation period to ensure that the probe no longer reacted with H_2S and the fluorescence intensity did not increase during the following process. After adding H_2S to the solution, the time-dependent fluorescence of

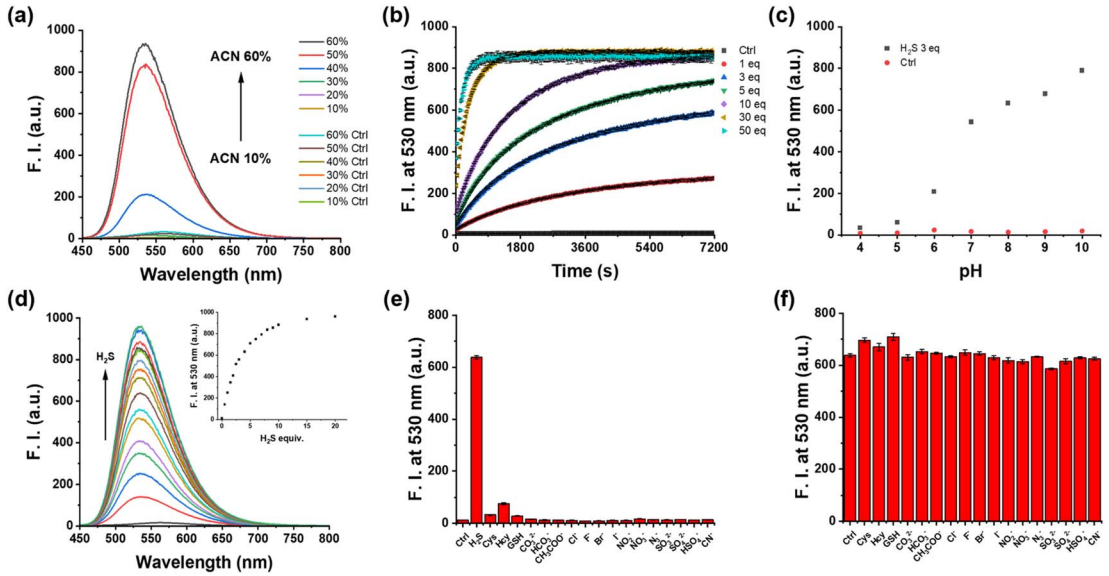

Fig. 1 Fluorescence emission spectra of **F-Naph-N$_3$** (20 μM) (a) with H_2S (10 eq.) in different ratio of ACN/H_2O solution (pH 8.0 sodium phosphate buffer (SPB) 10 mM) after 1 h [PMT: 580 V, slit: 5 nm] and (d) with various concentrations of H_2S (0–400 μM) in ACN/H_2O solution (v/v = 6 : 4, pH 8.0 SPB 10 mM) after 1 h. [PMT: 580 V, slit: 5 nm] (b) time-dependent fluorescent intensity of **F-Naph-N$_3$** (20 μM) at 530 nm in the absence and presence of H_2S in ACN/H_2O solution (v/v = 6 : 4, pH 8.0 SPB 10 mM) after 1 h. [PMT: 580 V, slit: 5 nm] (c) the plot of fluorescence intensity at 530 nm of **F-Naph-N$_3$** (20 μM) in the absence and presence of H_2S (3 eq.) in ACN/H_2O solution (v/v = 6 : 4, various pH range of buffer 10 mM) after 1 h. [PMT: 600 V, slit: 5 nm] (e) selectivity of **F-Naph-N$_3$** (20 μM) in ACN/H_2O solution (v/v = 6 : 4, pH 8.0 SPB 10 mM) in the presence of various analytes (100 μM) after 1 h: (1) control, (2) H_2S, (3) Cys, (4) Hcy, (5) GSH, (6) CO_3^{2-}, (7) HCO_3^-, (8) CH_3COO^-, (9) Cl^-, (10) F^-, (11) Br^-, (12) I^-, (13) NO_2^-, (14) NO_3^-, (15) N_3^-, (16) SO_3^{2-}, (17) SO_4^{2-}, (18) HSO_4^-, (19) CN^-. [PMT: 580 V, slit: 5 nm] (f) competitive selectivity of **F-Naph-N$_3$** (20 μM) with H_2S (100 μM) in ACN/H_2O solution (v/v = 6 : 4, pH 8.0 SPB 10 mM) in the presence of various analytes (300 μM) after 1 h: same as in (e). [PMT: 580 V, slit: 5 nm], λ_{ex} = 418 nm, at room temperature.

F-Naph-N$_3$ was measured for 1 h. Subsequently, copper(II) nitrate trihydrate, $Cu(NO_3)_2 \cdot 3H_2O$ was added (2 eq. of added H_2S, 2 vol%) to identify the quenching effect. As shown in Fig. S3,† the increase in fluorescence intensity instantly stopped and remained for an additional 30 min, confirming that copper nitrate can effectively quench the reaction by scavenging the remaining H_2S.

Based on the results obtained in the solution state, **F-Naph-N$_3$** was applied to F-SPE using a commercially available PTFE membrane filter. The sample was spotted onto the PTFE membrane and monitored using a hand-held UV lamp. Notably, the sample spots on the PTFE membrane filter induced strong fluorescence intensity, depending on the concentration of H_2S (Fig. S4† and 2a). To further validate this trend, a titration experiment using F-SPE procedure with PTFE filter was conducted. ChemiDoc MP imager (Bio-Rad) was used to obtain the fluorescence image of the sample, and Adobe Photoshop was used to convert the fluorescence into an optical density value. The fluorescence intensity showed a good linear correlation with H_2S even after two aqueous washes, showing the detection limit to be *ca.* 0.21 μM (Fig. 2b and S5†). According to the previously reported studies, fluorine atom basically disfavors other atoms due to its distinctive properties such as inert and amphiphobicity.[32] In addition, it results in that fluorous compounds, including fluorous-tagged substrates, generally favor fluorous phases instead of organic and aqueous phases, and various purification methods have been developed through these phenomena using PTFE materials.[25,26] These imply that **F-Naph-N$_3$** can be well absorbed on the PTFE material, and our result appropriately correlated the expected tendencies. As

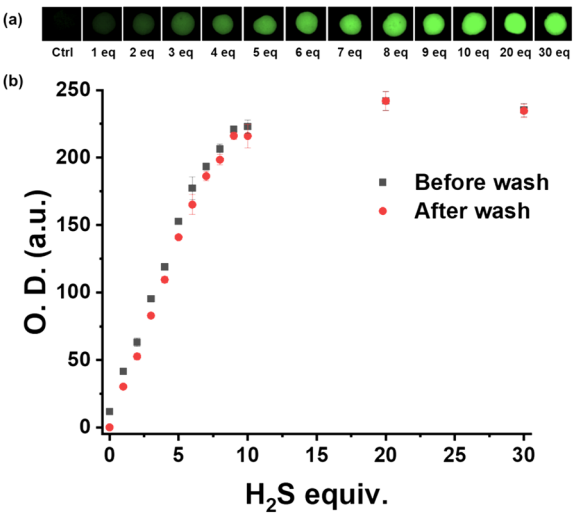

Fig. 2 (a) Fluorescence image of **F-Naph-N$_3$** spotted on polytetrafluoroethylene (PTFE) membrane filter. (b) **F-Naph-N$_3$** (20 μM) was spotted on PTFE membrane filter after 1 h incubation with the different concentration of H_2S (0–600 μM) in an ACN/H_2O solution (v/v = 6 : 4, pH 8.0 sodium phosphate buffer 10 mM), and the fluorescent intensity (optical density) of spots were measured before and after aqueous wash.

Table 1 Determination of H_2S in dyes-containing samples[a]

Sample	Added H_2S (μM)	Recovery[c] (%)	RSD (%)
Alizarin red S	20.0	107.8	13.1
	40.0	94.7	5.1
	60.0	97.8	14.1
Bromophenol blue	20.0	106.3	4.1
	40.0	99.6	10.1
	60.0	100	3.8
Methyl orange	20.0	109.2	2.1
	40.0	100.2	6.3
	60.0	101	7.4
Triple mixture[b]	20.0	111.3	10.9
	40.0	92.5	13.8
	60.0	97.5	9.5

[a] Condition: **F-Naph-N_3** (20 μM) was spotted on PTFE membrane filter after 1 h incubation with the different concentration of H_2S (20, 40, 60 μM) in an ACN/H_2O solution (v/v = 6 : 4, pH 8.0 sodium phosphate buffer 10 mM) containing 150 μM of organic dyes, and then the fluorescent intensity (optical density) of spots were measured. [b] Triple mixture sample consisted of 50 μM of three dyes. [c] Recovery rate was calculated as follows: [(intensity at samples)/(intensity at standard curve)] × 100%.

a result, it was demonstrated that the fluorescence of the probe could be selectively measured after F-SPE, indicating its potential for independent detection in the presence of interfering species.

3.5 Application for turbid dyeing solutions

Because the probe was designed to quantitatively detect H_2S in an opaque solution, F-SPE using **F-Naph-N_3** was examined in four organic dye solutions with different concentrations of H_2S. The fluorescence intensity of the probe was measured in 150 μM of each organic dye (Alizarin red S, Bromophenol blue, and Methyl orange), and their triple mixture (mixing three dyes of 50 μM) solutions. In Fig. S6,† the dashed line represents the standard values previously measured without any interfering species. As expected, the fluorescence of the dyeing solutions did not reach the standard value, indicating that their detection by fluorescence spectrometer is challenging due to the turbid environment. However, our fluorous-tagging strategy using **F-Naph-N_3** successfully enabled the detection of H_2S in the dyeing solution by effectively eliminating interfering organic dyes and other species through aqueous wash, as shown in Scheme 1b. Therefore, it was demonstrated that **F-Naph-N_3** can effectively detect H_2S levels in challenging turbid solutions (Table 1).

4 Conclusions

In summary, a fluorous-tag-assisted naphthalimide derivative, **F-Naph-N_3** was developed as a fluorescent probe to detect H_2S quantitatively. The interference effects of various anions and biothiols were almost negligible, indicating that **F-Naph-N_3** has good selectivity for H_2S in solution. Furthermore, it is noted that **F-Naph-N_3** could be easily isolated on the PTFE filter, and the other species were eliminated by a simple aqueous wash. As a result, the innovative fluorous-tagging strategy suggested in this work allows for accurate detection of H_2S concentrations even in highly turbid and deep-coloured dyeing solution. This protocol successfully overcomes the limitations of fluorescent probes in challenging environments and provides potential application to extended range of real samples.

Author contributions

Geonwoo Park: methodology, investigation, visualization, writing – original draft. Mincheol Jang: methodology, investigation, visualization, writing – original draft. Min Su Han: conceptualization, writing – review & editing, project administration.

Conflicts of interest

There are no conflicts to declare.

Acknowledgements

This work was supported by the National Research Foundation of Korea (NRF) grant funded by the Korea government (MSIT) (RS-2023-00247332 and RS-2023-00259685).

References

1 L. Long, S. Cao, B. Jin, X. Yuan, Y. Han and K. Wang, *Food Anal. Methods*, 2019, **12**, 852–858.
2 Y. Chen, C. Zhu, Z. Yang, J. Chen, Y. He, Y. Jiao, W. He, L. Qiu, J. Cen and Z. Guo, *Angew. Chem.*, 2013, **52**, 1688–1691.
3 C. Szabó, *Nat. Rev. Drug Discovery*, 2007, **6**, 917–935.
4 Y. S. Kafuti, S. Zeng, X. Liu, J. Han, M. Qian, Q. Chen, J. Wang, X. Peng, J. Yoon and H. Li, *Chem. Commun.*, 2023, **59**, 2493–2496.
5 B. Yu, C. Chen, J. Ru, W. Luo and W. Liu, *Talanta*, 2018, **188**, 370–377.
6 R. G. Hendrickson, A. Chang and R. J. Hamilton, *Am. J. Ind. Med.*, 2004, **45**, 346–350.
7 S. Arsawiset and S. Teepoo, *Anal. Chim. Acta*, 2020, **1118**, 63–72.
8 Y. Feng, S. Hu, Y. Wang, X. Song, C. Cao, K. Wang, C. Jing, G. Zhang and W. Liu, *J. Hazard. Mater.*, 2021, **406**, 124523.
9 V. Vitvitsky and R. Banerjee, *Methods Enzymol.*, 2015, **554**, 111–123.
10 L. A. Montoya, T. F. Pearce, R. J. Hansen, L. N. Zakharov and M. D. Pluth, *J. Org. Chem.*, 2013, **78**, 6550–6557.
11 Y. Zhao, Y. Yang, L. Cui, F. Zheng and Q. Song, *Biosens. Bioelectron.*, 2018, **117**, 53–59.
12 Z. Xu, L. Xu, J. Zhou, Y. Xu, W. Zhu and X. Qian, *Chem. Commun.*, 2012, **48**, 10871–10873.
13 D. Gong, X. Zhu, Y. Tian, S.-C. Han, M. Deng, A. Iqbal, W. Liu, W. Qin and H. Guo, *Anal. Chem.*, 2017, **89**, 1801–1807.
14 B. Gu, W. Su, L. Huang, C. Wu, X. Duan, Y. Li, H. Xu, Z. Huang, H. Li and S. Yao, *Sens. Actuators, B*, 2018, **255**, 2347–2355.

15 S. Y. Park, S. A. Yoon, Y. Cha and M. H. Lee, *Coord. Chem. Rev.*, 2021, **428**, 213613.
16 T. Lu, Z. Lin, J. Ren, P. Yao, X. Wang, Z. Wang and Q. Zhang, *PLoS One*, 2016, **11**, e0149751.
17 L. C. Zanetti-Domingues, C. J. Tynan, D. J. Rolfe, D. T. Clarke and M. Martin-Fernandez, *PLoS One*, 2013, **8**, e74200.
18 T.-W. Wu, F.-H. Lee, R.-C. Gao, C. Y. Chew and K.-T. Tan, *Anal. Chem.*, 2016, **88**, 7873–7877.
19 Y.-S. Zeng, R.-C. Gao, T.-W. Wu, C. Cho and K.-T. Tan, *Bioconjugate Chem.*, 2016, **27**, 1872–1879.
20 S. Yoo and M. S. Han, *Chem. Commun.*, 2019, **55**, 14574–14577.
21 X. Zhao, W. Zheng, T. Qin, X. Du, Y. Lei, T. Lv, M. Zhou, Z. Xu, L. Wang, B. Liu and X. Peng, *Sens. Actuators, B*, 2022, **351**, 130980.
22 Y. Chen, Z.-P. Chen, J. Yang, J.-W. Jin, J. Zhang and R.-Q. Yu, *Anal. Chem.*, 2013, **85**, 2015–2020.
23 H. Yu, F. Qu, Z. Wu, J. He, H. Rong and H. Liang, *Water Res.*, 2020, **187**, 116452.
24 Q. Zhang, Z. Luo and D. P. Curran, *J. Org. Chem.*, 2000, **65**, 8866–8873.
25 Y. Feng, J. Wu, G. Chen and Y. Chai, *Org. Lett.*, 2020, **22**, 2564–2568.
26 L. Cai, Q. Chen, J. Guo, Z. Liang, D. Fu, L. Meng, J. Zeng and Q. Wan, *Chem. Sci.*, 2022, **13**, 8759–8765.
27 R. L. Nicholson, M. L. Ladlow and D. R. Spring, *Chem. Commun.*, 2007, **38**, 3906–3908.
28 D. P. Curran, S. Hadida and M. He, *J. Org. Chem.*, 1997, **62**, 6714–6715.
29 Y.-Y. Zhu, X.-D. Wu, M. Abed, S.-X. Gu and L. Pu, *Chem.–Eur. J.*, 2019, **25**, 7866–7873.
30 P. Xiao, J. Liu, Z. Wang, F. Tao, L. Yang, G. Yuan, W. Sun and X. Zhang, *Chem. Commun.*, 2021, **57**, 5012–5015.
31 H.-Q. Dong, T.-B. Wei, X.-Q. Ma, Q.-Y. Yang, Y.-F. Zhang, Y.-J. Sun, B.-B. Shi, H. Yao, Y.-M. Zhang and Q. Lin, *J. Mater. Chem. C*, 2020, **8**, 13501–13529.
32 M. Cametti, B. Crousse, P. Metrangolo, R. Milani and G. Resnati, *Chem. Soc. Rev.*, 2012, **41**, 31–42.